

## Electron Scattering and Dissociative Attachment by SF<sub>6</sub> and Its Electrical-Discharge By-products

H.-X. Wan,<sup>1</sup> J. H. Moore,<sup>1</sup> J. K. Olthoff,<sup>2</sup>  
and R. J. Van Brunt<sup>2</sup>

Received December 2, 1991; revised June 15, 1992

---

*Discrete electron-molecule processes relevant to SF<sub>6</sub> etching plasmas are examined. Absolute, total scattering cross sections for 0.2-12-eV electrons on SF<sub>6</sub>, SO<sub>2</sub>, SOF<sub>2</sub>, SO<sub>2</sub>F<sub>2</sub>, SOF<sub>4</sub>, and SF<sub>4</sub>, as well as cross sections for negative-ion formation by attachment of electrons, have been measured. These are used to calculate dissociative-attachment rate coefficients as a function of E/N for SF<sub>6</sub> by-products in SF<sub>6</sub>.*

---

**KEY WORDS:** Attachment rates; cross section; dissociative attachment; electron scattering; SF<sub>6</sub>, SF<sub>4</sub>, SO<sub>2</sub>, SOF<sub>2</sub>, SOF<sub>4</sub>, SO<sub>2</sub>F<sub>2</sub>.

### 1. INTRODUCTION

Sulfur hexafluoride (SF<sub>6</sub>) is used as an insulating medium in high-voltage power transmission devices<sup>(1)</sup> and as an etchant in the plasma processing of microelectronic devices.<sup>(2-7)</sup> The silicon etching rates in SF<sub>6</sub> plasmas are comparable to or greater than those in CF<sub>4</sub> plasmas.<sup>(2,3)</sup> The addition of small amounts of O<sub>2</sub> to an SF<sub>6</sub> plasma reduces the lateral etch rate, thus greatly increasing etching anisotropy.<sup>(5)</sup> Plasmas in SF<sub>6</sub>/O<sub>2</sub> mixtures are quite complex, yielding large quantities of gaseous by-products.<sup>(6,7)</sup> Under some conditions in an SF<sub>6</sub>/O<sub>2</sub> plasma, over 20 mole % of the neutral species are decomposition products such as SO<sub>2</sub>, SOF<sub>2</sub>, SO<sub>2</sub>F<sub>2</sub>, SOF<sub>4</sub>, and SF<sub>4</sub>.<sup>(8)</sup>

Clearly, an understanding of the physical processes occurring in SF<sub>6</sub> plasmas requires a knowledge of the manner in which electrons interact with the decomposition by-products of SF<sub>6</sub>. Cross sections and rate coefficients for such interactions are essential for the modeling of SF<sub>6</sub> etching

<sup>1</sup> Department of Chemistry and Biochemistry, University of Maryland, College Park, Maryland 20742.

<sup>2</sup> National Institute of Standards and Technology, Gaithersburg, Maryland 20899.

plasmas.<sup>(4)</sup> A dearth of such information has led us to undertake measurements of absolute cross sections for total electron scattering and for negative-ion formation through electron attachment to SF<sub>6</sub> and to SO<sub>2</sub>, SOF<sub>2</sub>, SO<sub>2</sub>F<sub>2</sub>, SOF<sub>4</sub>, and SF<sub>4</sub>, all of which are commonly produced by electrical discharges in SF<sub>6</sub>. These results are compared with previous cross-section measurements (where available) and with mass-spectrometric studies for ion identification. Dissociative-attachment rate coefficients for the SF<sub>6</sub> decomposition products in SF<sub>6</sub> are calculated as a function of electric field-to-gas-density ratio ( $E/N$ ) using the cross sections reported here. The range of  $E/N$  values considered here is that which applies to electrical-discharge conditions.

## 2. EXPERIMENT

An electron transmission spectrometer employing a trochoidal monochromator<sup>(9)</sup> forms the basis of the experimental apparatus. This instrument consists of a thermionic electron source followed by the trochoidal monochromator, an accelerating lens, a gas cell, and a retarding lens which permits only unscattered electrons to be transmitted to an electron collector. The instrument is immersed in a uniform magnetic field of about 7 mT (70 G). The electron-energy resolution ranged from 50 to 80 meV, depending upon operating conditions, and the temperature within the scattering region was maintained at 328 K. A determination of the energy scale was made by observing the vibrational structure of the  $^2\Pi_g$  shape resonance in N<sub>2</sub> centered around 2.3 eV. The estimated uncertainty is <50 meV over the entire energy range considered. Total electron-scattering cross sections are obtained by measuring the attenuation of the transmitted current due to the introduction of a sample into the gas cell.<sup>(10)</sup> Cross sections for electron attachment yielding metastable negative ions (lifetimes >10  $\mu$ s) and dissociative-attachment processes are determined from a measurement of the product negative ion flux to the walls of the gas cell.<sup>(11)</sup> More detailed experimental descriptions have been published elsewhere.<sup>(10,11)</sup>

The presence of the magnetic field introduces uncertainty in the length of the electron trajectories through the gas cell<sup>(10)</sup> as well as uncertainty in the acceptance angle defined by the retarding lens which precedes the collector.<sup>(12)</sup> Additional uncertainty is associated with the measurement of the target gas pressure in the 0.03–0.13 Pa (0.2–1.0 mtorr) range at which the cross sections were determined. Overall, the cross sections reported are believed to be accurate to within  $\pm 15\%$  for electron energies above 1 eV. Below this energy, the uncertainty may increase to as much as  $\pm 50\%$  at the lowest energies ( $\leq 0.2$  eV). Measurement of cross sections for well-characterized gases, such as N<sub>2</sub> and N<sub>2</sub>O, indicate that discrepancies between values

obtained with this technique and other previously reported values are less than these estimated uncertainties. Due to adverse interactions of sulfur-containing species with the electron source, the limit of sensitivity in the dissociative-attachment cross section measurements varied with each compound, but was typically better than  $2 \times 10^{-18} \text{ cm}^2$ .

The SF<sub>6</sub>, SO<sub>2</sub>, SOF<sub>2</sub>, and SO<sub>2</sub>F<sub>2</sub> samples were obtained from commercial sources and were used without further purification. The SOF<sub>4</sub> and SF<sub>4</sub> samples were prepared by Dr. D. DeMarteau (Clemson University) with stated purities of >99%. The purities of all samples were checked by mass spectrometry and GC/MS.

### 3. EXPERIMENTAL RESULTS AND DISCUSSION

#### 3.1. SF<sub>6</sub>

The present measurement of the total electron-scattering cross section for SF<sub>6</sub> is shown in Fig. 1 and is compared with previous measurements.<sup>(13-15)</sup> Above 0.5 eV, all of the measurements agree to within 10%. Below 0.5 eV, the values from the present work fall systematically below the cross sections

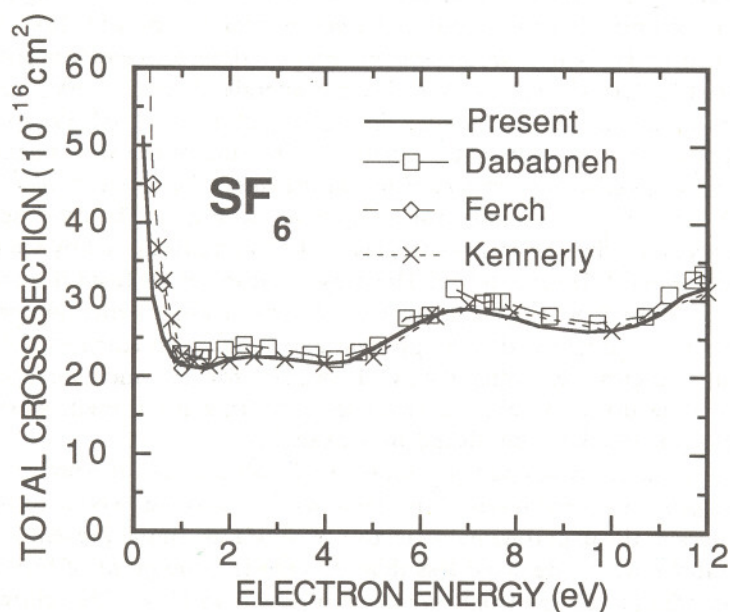


Fig. 1. Total electron-scattering cross sections for SF<sub>6</sub> as measured by the present experiment compared with previous measurements by Dababneh *et al.*,<sup>(14)</sup> Ferch *et al.*,<sup>(15)</sup> and Kennerly *et al.*<sup>(13)</sup>

reported by Kennerly *et al.*<sup>(13)</sup> and Ferch *et al.*<sup>(15)</sup> This may be due to the use in this experiment of a retarding potential filter to reject scattered electrons. The acceptance angle of a retarding potential filter increases with decreasing energy, most markedly at very low energies.

Negative-ion formation by electron attachment and dissociative attachment to SF<sub>6</sub> has been the subject of intensive study.<sup>(16,17)</sup> Christophorou and coworkers<sup>(18)</sup> have performed several swarm studies of electron attachment to SF<sub>6</sub>, and Fenzloff *et al.*<sup>(19)</sup> have published a detailed study of the relative ion yields for dissociative attachment to SF<sub>6</sub>. At very low energies (0–0.2 eV), Chutjian and coworkers<sup>(20)</sup> have measured absolute attachment cross sections using threshold photoemission as an electron source. Kline and coworkers<sup>(21)</sup> have measured cross sections for attachment and dissociative attachment to SF<sub>6</sub> from 0.01 to 15 eV in a beam experiment where the absolute magnitudes were determined by comparison with various positive-ion cross sections and normalizing with respect to total ionization cross-section measurements.<sup>(22)</sup> More recently, Hunter and coworkers<sup>(23)</sup> have calculated cross sections for attachment and dissociative attachment to SF<sub>6</sub> using attachment rates measured in swarm experiments using extremely diluted mixtures of SF<sub>6</sub> in N<sub>2</sub>, Ar, and Xe. Differences between the dissociative-attachment cross section measurements exceed an order-of-magnitude.

The combined cross section for electron attachment and dissociative attachment to SF<sub>6</sub> is measured in the present experiment for electron energies from 0.04 to 1.1 eV (Fig. 2). For electron energies below 0.2 eV, electron attachment is dominated by SF<sub>6</sub><sup>-</sup> formation, and above 0.2 eV, by SF<sub>5</sub><sup>-</sup> formation from dissociative attachment.<sup>(19)</sup> The sum of the attachment and dissociative-attachment cross sections as measured by Kline *et al.*<sup>(21)</sup> and by Hunter *et al.*<sup>(23)</sup> are shown for comparison in Fig. 2. The cross section for electron attachment at low energies (<0.2 eV) as measured by Chutjian and coworkers<sup>(20)</sup> is also shown. The cross section values from the present work are in reasonable agreement with previous measurements for energies less than 0.1 eV and are also in apparent agreement with Kline *et al.*<sup>(21)</sup> for electron energies exceeding 0.4 eV. However, for intermediate energies ranging from 0.1 to 0.4 eV, the cross sections from the present work significantly exceed those published previously.<sup>(21,23)</sup>

The apparent discrepancy from 0.1 to 0.4 eV between the present data and the previously published cross sections<sup>(21,23)</sup> may be explained by the differences in the experimental detection procedures. In the present experiment, most ions are detected less than 0.5 cm from the point of formation corresponding to a time from formation of less than 10 μs. This allows for the collection of SF<sub>6</sub><sup>-</sup> ions that are formed in excited states with relatively short lifetimes. Evidence suggests that these lifetimes range in length from a few microseconds to milliseconds.<sup>(24)</sup> Ions formed in excited states of SF<sub>6</sub><sup>-</sup>

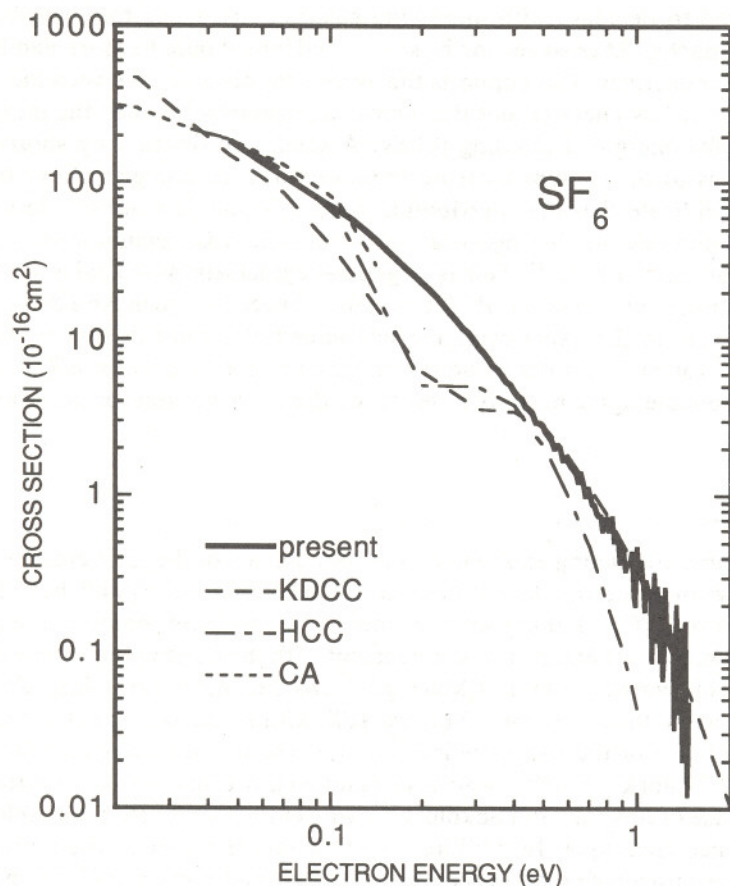


Fig. 2. Cross sections for attachment and dissociative attachment to SF<sub>6</sub> as compared with previous measurements by Kline, Davis, Chen, and Chantry,<sup>(21)</sup> Hunter, Carter, and Christophorou,<sup>(23)</sup> and Chutjian and Alajajian.<sup>(20)</sup>

with short lifetimes may not be detected in the experiment of Kline and coworkers<sup>(21)</sup> because the mass analysis requires ion transit times longer than 10  $\mu$ s before detection, resulting in a lower measured effective cross section for SF<sub>6</sub><sup>-</sup> formation. In the drift-tube experiment of Hunter *et al.*<sup>(23)</sup> the detected SF<sub>6</sub><sup>-</sup> ions have been collisionally stabilized under relatively high-pressure drift conditions in rare gases. Under these conditions there may also be discrimination against short-lived SF<sub>6</sub><sup>-</sup> in excited states. It has been shown<sup>(25)</sup> that electrons are more readily detached from excited states of SF<sub>6</sub><sup>-</sup> by collisions with rare gas atoms, thus destroying those ions before they can be detected in the drift tube. The lifetimes of excited SF<sub>6</sub><sup>-</sup> are

expected to decrease with increasing electron energy, so the contribution to the attachment cross section by short-lived ions should be more significant at higher energies. This supports the agreement observed between the cross sections at low energies and the increasing disparity between the measurements for energies exceeding 0.1 eV. A small contribution by short-lived  $SF_6^-$  ions to the present measure cross sections for energies above 0.4 eV would indicate that the contribution from  $SF_5^-$  ion formation is less than that implied by the  $SF_5^-$  dissociative-attachment cross section measured by Kline and coworkers.<sup>(21)</sup> This is in general agreement with analyses<sup>(23,26-28)</sup> of electron swarm data for which it was found necessary to make a downward adjustment in the experimentally determined electron-collision cross sections<sup>(11)</sup> for  $SF_5^-$  in order to obtain attachment coefficients for  $SF_6$  that are in reasonable agreement with results of the most accurate measurements.

### 3.2. $SO_2$

Three conflicting experimental measurements of the total cross section for electron scattering by sulfur dioxide ( $SO_2$ ) have been published. These are shown in Fig. 3 along with the measurements from the present experiment. Our results are in closest agreement with the transmission experiment results of Szmytkowski and Maciag.<sup>(29)</sup> Discrepancies exceeding 20% are observed at lower energies but are still within the combined estimated uncertainties of the two experiments. Our results are clearly at odds with those of Zubek *et al.*<sup>(30)</sup> who also employed a transmission experiment, and those of Sokolov and Sokolova<sup>(31)</sup> who employed an electron cyclotron resonance technique. In addition, we find that the sum of the ionization and elastic scattering cross sections of Orient and coworkers<sup>(32,33)</sup> and the electronic excitation cross sections of Vušković and Trajmar<sup>(34)</sup> falls significantly below our total electron-scattering cross section.

The broad maximum observed in the total cross section near 5 eV corresponds to the second resonance observed by Sanche and Schulz<sup>(35)</sup> in the electron transmission spectrum. A resonance near 3.4 eV observed by Sanche and Schulz<sup>(35)</sup> and by Andrić *et al.*<sup>(36)</sup> is not evident in the total cross section.

As can be seen from the lower curves in Figure 3, previous measurements of the cross sections for dissociative attachment to  $SO_2$  differ somewhat in magnitude from those reported here. Čadež and coworkers<sup>(37)</sup> measured total dissociative-attachment cross sections using a transmission experiment similar to that described in this paper. Orient and Srivastava<sup>(38)</sup> measured mass-resolved dissociative-attachment cross sections in a beam experiment with normalization of the measured  $O^-/SO_2$  cross section to

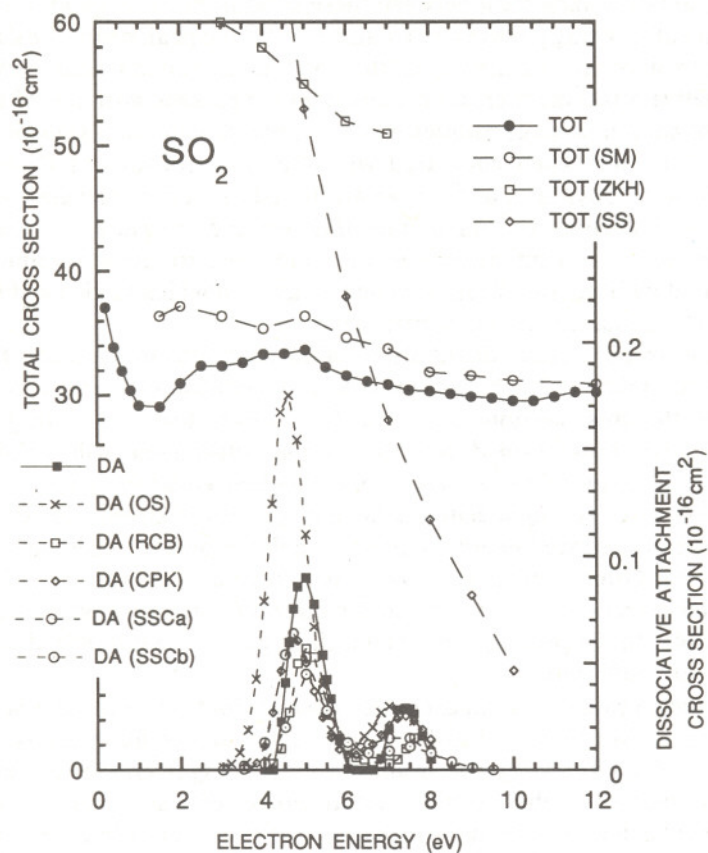


Fig. 3. Total electron-scattering cross sections (upper curves, left ordinate) and dissociative-attachment cross sections (lower curves, right ordinate) for SO<sub>2</sub> as compared with previous measurements: SM<sup>(29)</sup>; ZKH<sup>(30)</sup>; SS<sup>(31)</sup>; OS<sup>(33)</sup>; RCB<sup>(40)</sup>; CPK<sup>(37)</sup>; SSCa,<sup>(29)</sup> time-of-flight measurement; SSCb,<sup>(39)</sup> swarm measurement.

the well-known O<sup>-</sup>/O<sub>2</sub> cross section. The magnitude of the sum of the mass-resolved cross sections exceeds that of the total cross section measured by Čadež and coworkers<sup>(37)</sup> by a factor of 3. Spyrou *et al.*<sup>(39)</sup> also carried out a mass-analyzed beam experiment, but determined the magnitude of the cross section by comparison with the production of F<sup>-</sup> from C<sub>2</sub>F<sub>6</sub>. Their results are in good agreement with Čadež *et al.* In the same paper, Spyrou *et al.* also reported the total dissociative-attachment cross section using a swarm-beam technique which gave magnitudes lower than the beam experiments but in good agreement with early swarm experiments of Rademacher *et al.*<sup>(40)</sup>

Qualitative agreement between these measurements is good, with each experiment showing peaks near 4.7 and 7.2 eV. The peak near 4.7 eV corresponds to a broad maximum in the total cross section near 5 eV. The dissociative-attachment cross sections from the present work are within the limits of combined uncertainties when compared with the results of Čadež *et al.*<sup>(37)</sup> but not when compared with the cross sections of Orient and Srivastava.<sup>(38)</sup> Spyrou *et al.*<sup>(39)</sup> have attributed the inconsistencies between the SO<sub>2</sub> dissociative-attachment data of Orient and Srivastava and the other dissociative-attachment measurements to mass-spectrometer discrimination associated with the significant kinetic energy with which O<sup>-</sup> is produced in the O<sup>-</sup>/O<sub>2</sub> process used for normalization.

Anisotropic angular distributions of the negative-ion fragments formed in the dissociative-attachment process can contribute to inconsistencies between the cross sections measured by different techniques. In general, the negative ions formed by dissociative attachment will exhibit an anisotropic distribution relative to the incident electron beam.<sup>(41,42)</sup> The formation of O<sup>-</sup> by dissociative attachment of O<sub>2</sub> is known, for example, to exhibit pronounced energy-dependent anisotropies.<sup>(43)</sup> Techniques such as used by Orient and Srivastava<sup>(38)</sup> that restrict observation of ions to preferred directions relative to the direction of electron motion are most susceptible. In the present experiment, these effects are minimized because all ions are collected.

In recent calculations of excitation energies for transitions of inner-shell electrons to low-lying unfilled orbitals in the sulfur fluorides and oxyfluorides, Tossell<sup>(44,45)</sup> has been able to make assignments of the unfilled orbitals involved in the electron-capture processes leading to dissociative attachment. These results suggest that the 5-eV resonance in the total cross section and the corresponding dissociation are associated with electron capture into an *a*<sub>1</sub> orbital of SO<sub>2</sub>, the second-lowest, unfilled molecular orbital.

### 3.3. SOF<sub>2</sub>

Total electron-scattering and dissociative-attachment cross sections for thionyl fluoride (SOF<sub>2</sub>) are shown in Fig. 4. A prominent resonance in the total cross section at 0.6 eV corresponds to a peak in the dissociative-attachment cross section near 0.7 eV. These processes have been assigned to electron capture into the *a*'' lowest unoccupied molecular orbital (LUMO) of SOF<sub>2</sub>.<sup>(44)</sup> A weaker resonance in the total cross section near 2 eV corresponds to a shoulder in the dissociative-attachment cross section near 1.8 eV. Mass-spectrometric studies<sup>(46)</sup> find an F<sup>-</sup> peak near 0.6 eV with a small shoulder near 2 eV, in agreement with the present cross sections. For electron

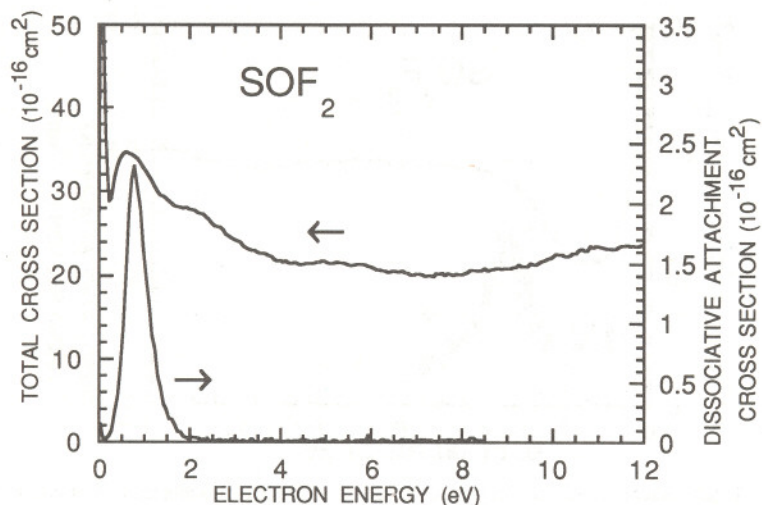


Fig. 4. Total electron-scattering (upper curve) and dissociative-attachment (lower curve) cross sections for  $\text{SOF}_2$ .

energies near 0 eV, Sauer *et al.*<sup>(46)</sup> have observed the formation of  $\text{SOF}_2^-$  at peak intensities approximately 200 times smaller than for  $\text{F}^-$ . This small current would be undetectable in the present experiment.

### 3.4. $\text{SO}_2\text{F}_2$

Figure 5 shows the cross sections for electron scattering and dissociative attachment by sulfurylfluoride ( $\text{SO}_2\text{F}_2$ ). The total cross section exhibits a broad shoulder near 3 eV corresponding to a peak in the dissociative-attachment cross section near 3.4 eV. These features have been assigned to the  $b_1$  LUMO of  $\text{SO}_2\text{F}_2$ . The peak in the dissociative-attachment cross section near 3.4 eV is in agreement with mass-spectrometric studies by Wang and Franklin<sup>(47)</sup> and by Sauer and coworkers.<sup>(46)</sup> These studies indicate that this peak corresponds to the formation of  $\text{SO}_2\text{F}^-$ ,  $\text{F}_2^-$ , and  $\text{F}^-$ , and that the increase in the attachment cross section at low energies is due to the formation of the parent ion,  $\text{SO}_2\text{F}_2^-$ . The low-energy electron-attachment cross section has been determined by Datskos and Christophorou<sup>(48)</sup> from electron-swarm measurements and shown to have a strong temperature dependence. For a temperature of 300 K, the  $\text{SO}_2\text{F}_2$  attachment cross section is reported to have a peak value of  $1.06 \times 10^{-16} \text{ cm}^2$  at 0.22 eV. The measured dissociative-attachment cross section from the present experiment shows no maximum at low energy and is approximately  $0.11 \times 10^{-16} \text{ cm}^2$  at 0.22 eV. This is significantly lower than the value obtained by Datskos *et al.*,<sup>(48)</sup> even

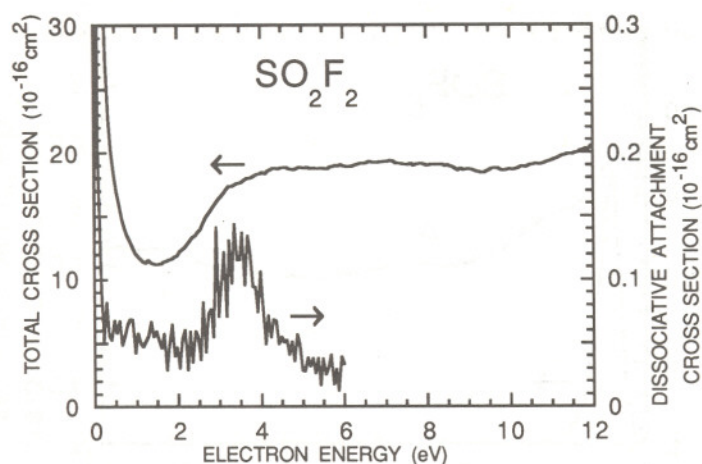


Fig. 5. Total electron-scattering (upper curve) and dissociative-attachment (lower curve) cross sections for  $\text{SO}_2\text{F}_2$ . The increase in the dissociative-attachment cross section at low energies is due to formation of the parent ion  $\text{SO}_2\text{F}_2^-$ .<sup>(46)</sup>

allowing for the larger uncertainties in the present measurements at lower electron energies.

### 3.5. $\text{SOF}_4$

The total electron-scattering and dissociative-attachment cross sections for thionyl tetrafluoride ( $\text{SOF}_4$ ) are shown in Fig. 6. Broad resonance features are observable in the total cross section near 3, 6, and 10 eV. Mass-spectrometric studies<sup>(46)</sup> have identified an  $\text{F}^-$  peak at 3.2 eV corresponding to the small peak near 3 eV in the dissociative-attachment cross section. The large dissociative-attachment cross section near 0 eV has been shown to correspond to  $\text{SOF}_3^-$  production.<sup>(46)</sup> It is of interest to note that the magnitude of the threshold dissociative-attachment cross section for  $\text{SOF}_4$  is comparable to the threshold electron-attachment cross section for  $\text{SF}_6$ .

### 3.6. $\text{SF}_4$

Total electron-scattering and dissociative-attachment cross sections for sulfur tetrafluoride ( $\text{SF}_4$ ) are presented in Fig. 7. A strong resonance is observable near 0.4 eV in the total scattering cross section, while the dissociative-attachment cross section exhibits a peak at 0.6 eV. These processes are associated with electron capture into the  $b_2$  LUMO of  $\text{SF}_4$ .<sup>(44)</sup> The dissociative-attachment peak is in agreement with  $\text{F}^-$  production observed in pre-

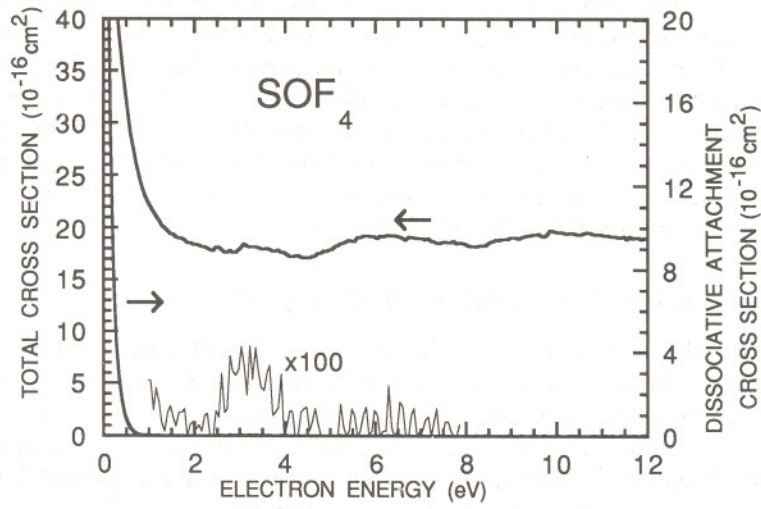


Fig. 6. Total electron-scattering (upper curve) and dissociative-attachment (lower curve) cross sections for SOF<sub>4</sub>.

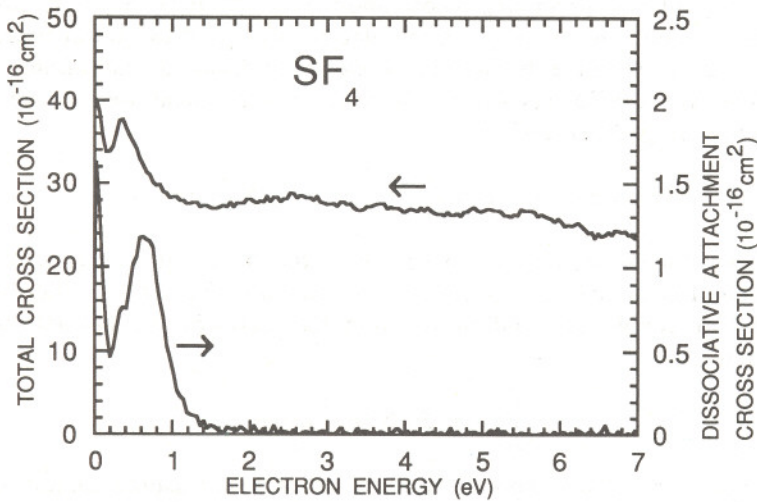


Fig. 7. Total electron-scattering (upper curve) and dissociative-attachment (lower curve) cross sections for SF<sub>4</sub>. The increase in the dissociative-attachment cross section at low energies is due to formation of the parent ion (SF<sub>4</sub><sup>-</sup>).

vious mass-spectrometric data.<sup>(46)</sup> The increase in the dissociative-attachment cross section at low energies is due to the formation of  $\text{SF}_4^-$ .<sup>(46)</sup> Previous studies have determined that the threshold electron-capture cross section for  $\text{SF}_4$  is two orders of magnitude smaller than for  $\text{SF}_6$ .<sup>(49,50)</sup> More recent data suggest that the threshold attachment rates differ by a factor of 10.<sup>(57)</sup> Although the present experiment does not extend down to thermal energies, our data indicate that the electron-capture cross sections for  $\text{SF}_4$  and  $\text{SF}_6$  differ by approximately a factor of 70 at 0.1 eV.

### DISSOCIATIVE ATTACHMENT RATES IN $\text{SF}_6$

The dissociative-attachment cross sections for  $\text{SF}_4$ ,  $\text{SO}_2$ ,  $\text{SO}_2\text{F}_2$ , and  $\text{SOF}_2$  reported in the previous section have been used to compute dissociative-attachment rate coefficients for these molecules as functions of electric field-to-gas density ratio in  $\text{SF}_6$ . It was assumed in making the calculations that these species are present at sufficiently low concentrations in  $\text{SF}_6$  that one is justified in using electron kinetic-energy distribution functions that apply to pure  $\text{SF}_6$ . This assumption is valid in cases where  $\text{SF}_6$  is only weakly decomposed in an electrical discharge as occurs in low-level corona or glow discharge.<sup>(52-54)</sup> The results obtained here will also apply under the conditions where  $\text{SF}_6$  is highly dissociated or decomposed provided the electron-energy distributions do not deviate significantly from those used here. It is known from previous calculations<sup>(26,55)</sup> that the presence of other electronegative gases in  $\text{SF}_6$  below about the 10% level has a relatively minor influence on the shape of the electron-energy distribution function if  $E/N$  is in the range that applies to electrical discharge conditions.

The rate coefficients  $k_d$  for dissociative attachment were computed using the integral expression

$$k_d(E/N) = (2/m_e)^{1/2} \int_0^\infty \epsilon f(\epsilon, E/N) \sigma_d(\epsilon) d\epsilon \quad (1)$$

where  $\epsilon$  is the electron kinetic energy,  $m_e$  is the mass of the electron,  $\sigma_d(\epsilon)$  is the net dissociative-attachment cross section, and  $f(\epsilon, E/N)$  is the  $E/N$ -dependent energy distribution function that satisfies the normalization requirement

$$\int_0^\infty f(\epsilon, E/N) \epsilon^{1/2} d\epsilon = 1 \quad (2)$$

In general,  $\sigma_d(\epsilon)$  corresponds to the sum of all measured dissociative-attachment cross sections of a given molecule for  $\epsilon > 0.2$  eV, i.e.,

$$\sigma_d(\epsilon) = \sum_i \sigma_{di}(\epsilon) \quad (3)$$

where, in performing the present calculations, the  $\sigma_{di}(\epsilon)$  were represented by Gaussian fits to the measured data corresponding to the different individual features. Dissociative-attachment processes with cross sections peaked at or near zero energy ( $\epsilon < 0.2$  eV) were not included in these calculations.

The kinetic energy distributions were computed from numerical solutions to the Boltzmann transport equation using a "two-term" approximation and the set of SF<sub>6</sub> electron collision cross sections proposed by Phelps and Van Brunt.<sup>(26)</sup> Examples of the computed energy-distribution functions multiplied by the energy,  $\epsilon f(\epsilon, E/N)$ , are shown in Fig. 8 for  $E/N$  in the range of  $150 \times 10^{-21}$  to  $1000 \times 10^{-21}$  V m<sup>2</sup>. It should be noted that the critical minimum value of  $E/N$  required to initiate and sustain a gas discharge in pure SF<sub>6</sub> is  $354 \times 10^{-21}$  V m<sup>2</sup>.<sup>3</sup> At this value of  $E/N$ , the ionization rate is comparable to the electron-attachment rate,<sup>(21,26)</sup> and  $\epsilon f(\epsilon, E/N)$  is peaked at about 8.0 eV. Thus, under gas-discharge conditions, it can be expected that dissociative-attachment processes that occur at electron energies above about 1 eV will contribute more disproportionately to negative-ion formation than processes at lower energies.

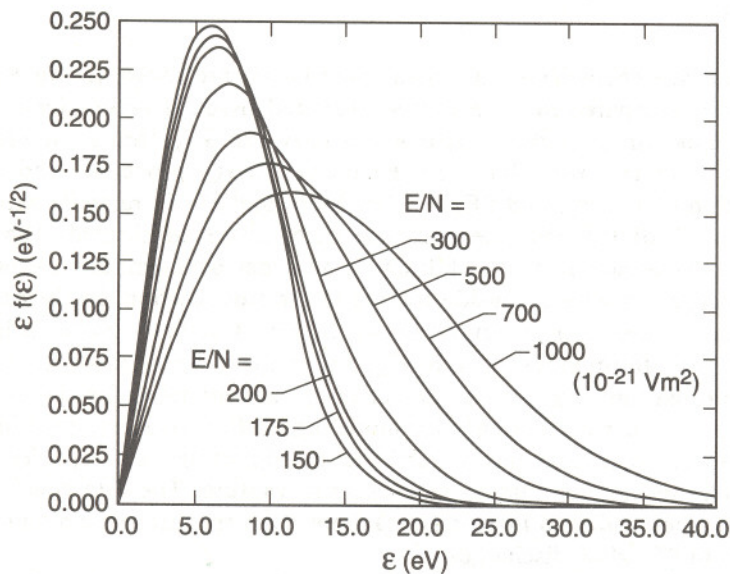


Fig. 8. Electron kinetic-energy distribution functions, calculated by the method discussed in Ref. 26, for electrons in pure SF<sub>6</sub> at different values of  $E/N$ .

<sup>3</sup> There is experimental evidence that the minimum  $E/N$  in a self-sustained SF<sub>6</sub> glow discharge is that at which the ionization rate equals the attachment rate.<sup>(56)</sup>

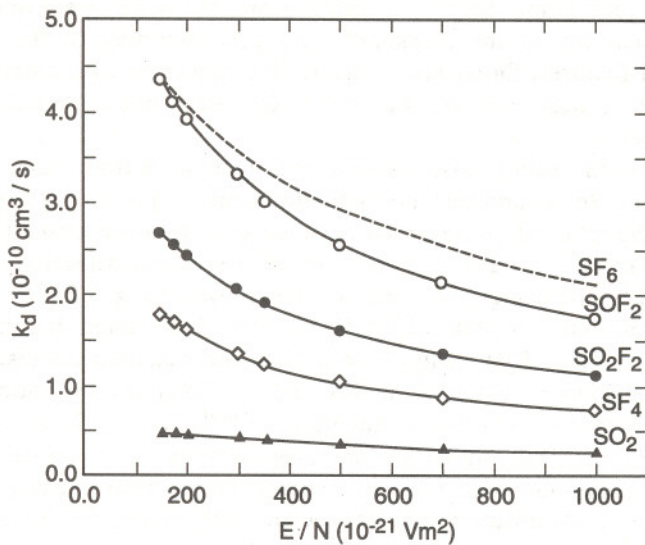


Fig. 9. Calculated total dissociative electron attachment rate coefficients for  $\text{SOF}_2$ ,  $\text{SO}_2\text{F}_2$ ,  $\text{SF}_4$ , and  $\text{SO}_2$  in  $\text{SF}_6$  as a function of  $E/N$ . The results for  $\text{SF}_6$  are the same as given in Refs. 26 and 55.

The rate coefficients calculated using Eq.(1) are shown in Fig. 9. The results are compared with previously calculated dissociative-attachment rate coefficients for  $\text{SF}_6$  which include not only the  $\text{SF}_5^-$  formation process examined in this work but also the higher energy processes leading to formation of  $\text{F}^-$ ,  $\text{F}_2^-$ , and  $\text{SF}_4^-$ .<sup>(55)</sup> The  $\text{SOF}_2$  and  $\text{SO}_2\text{F}_2$  rates lie within a factor of 2 of the  $\text{SF}_6$  rate over the  $E/N$  range considered. The  $\text{SO}_2$  dissociative-attachment rates fall about an order of magnitude below the  $\text{SF}_6$  rates, as expected, considering the lower cross section. In the case of  $\text{SO}_2$ , the higher energy feature shown in Fig. 3 actually makes a larger contribution to the rates given in Fig. 9 than the lower energy feature.

Information about the dissociative-attachment rates for the species considered is needed not only for modeling of discharge processes in  $\text{SF}_6$  but also for assessing the possibilities for detecting these species with analytical techniques that employ electron capture. The rate coefficients may also be needed to interpret data from mass spectrometric monitoring of ions in  $\text{SF}_6$  glow discharges.<sup>(7,8)</sup>

#### 4. CONCLUSIONS

Sulfur hexafluoride and its discharge by-products have comparable total electron-scattering cross sections at energies above threshold. By con-

trast, the magnitudes of the dissociative-attachment cross sections for these compounds vary over several orders of magnitude. The dissociative attachment rates for SOF<sub>2</sub>, SO<sub>2</sub>F<sub>2</sub>, and SF<sub>4</sub> are within a factor of three of the rate for SF<sub>6</sub> over a broad range of  $E/N$  applicable to gas charge conditions. It can thus be expected that the by-products in an SF<sub>6</sub> plasma are significant sources of negative ions and reactive radicals.

Temperature has a significant effect on the dissociative-attachment cross sections of SF<sub>6</sub>,<sup>(57)</sup> SO<sub>2</sub>,<sup>(39)</sup> and SO<sub>2</sub>F<sub>2</sub>.<sup>(48)</sup> Plasma temperatures are sometimes above room temperature, and thus the temperature dependence of the cross sections presented here should be considered. This will be the focus of future work.

#### ACKNOWLEDGMENT

This work was supported by NSF Grant No. CHE-91-20504 and the U.S. Department of Energy.

#### REFERENCES

1. F. Y. Chu, *IEEE Trans. Electr. Insul.* **EI-21**, 693 (1986); W. Rügsegger, R. Meier, F. K. Kneubühl, and H. J. Schötzau, *Appl. Phys. B* **37**, 115 (1985).
2. J. J. Wagner and W. W. Brandt, *Plasma Chem. Plasma Process.* **1**, 201 (1981); K. M. Eisele, *J. Electrochem. Soc.* **128**, 123 (1981); G. S. Oehrlein, K. K. Chan, M. A. Jaso, and G. W. Rubloff, *J. Vac. Sci. Technol. A* **7**, 1030 (1989).
3. S. Park, C. Sun, and R. J. Purtell, *J. Vac. Sci. Technol. B* **5**, 1372 (1987); L. E. Kline, *IEEE Trans. Plasma Sci* **14**, 145 (1986).
4. A. Picard, G. Turban, and B. Grolleau, *J. Phys. D* **19**, 991 (1986).
5. A. Manenschijn, G. C. A. M. Janssen, E. van der Drift, and S. Radelaz, *J. Appl. Phys.* **65**, 3226 (1989).
6. R. d'Agostino and D. L. Flamm, *J. Appl. Phys.* **52**, 162 (1981).
7. A. Picard, and G. Turban, *Plasma Chem. Plasma Process.* **5**, 333 (1985).
8. G. Turban and M. Rapeaux, *J. Electrochem. Soc.* **130**, 2231 (1983).
9. A. Stamatovic and G. J. Schulz, *Rev. Sci. Instrum.* **41**, 423 (1970); M. R. McMillan and J. H. Moore, *ibid.* **51**, 944 (1980); G. J. Schulz, *Phys. Rev. A* **5**, 1672 (1972).
10. H.-X. Wan, J. H. Moore, and J. A. Tossell, *J. Chem. Phys.* **91**, 7340 (1989).
11. H.-X. Wan, J. H. Moore, and J. A. Tossell, *J. Chem. Phys.* **94**, 1868 (1991).
12. A. R. Johnston and P. D. Burrow, *J. Electron Spectrosc. Relat. Phenom.* **25**, 119 (1982).
13. R. E. Kennerly, R. A. Bonham, and M. McMillan, *J. Chem. Phys.* **70**, 2039 (1979).
14. M. S. Dababneh, Y.-F. Hsieh, W. E. Kaupilla, C. K. Kwan, S. J. Smith, T. S. Stein, and M. N. Uddin, *Phys. Rev. A* **38**, 1207 (1988).
15. J. Ferch, W. Raith and K. Schröder, *J. Phys. B* **15**, L175 (1982).
16. F. C. Fehsenfeld, *J. Chem. Phys.* **53**, 2000 (1970).
17. P. J. Hay, *J. Chem. Phys.* **76**, 502 (1982).
18. L. G. Christophorou, D. L. McCorkle, and J. G. Carter, *J. Chem. Phys.* **54**, 253 (1971); D. L. McCorkle, A. A. Christodoulides, L. G. Christophorou, and I. Szamrej, *ibid.*, **72**, 4049 (1980).

19. M. Fenzloff, R. Gehard, and E. Illenberger, *J. Chem. Phys.* **88**, 149 (1988).
20. A. Chutjian and S. H. Alajajian, *Phys. Rev. A* **31**, 2885 (1985); O. J. Orient and A. Chutjian, *ibid.* **34**, 1841 (1986).
21. L. E. Kline, D. K. Davis, C. L. Chen, and P. J. Chantry, *J. Appl. Phys.* **50**, 6789 (1979).
22. D. Rapp and P. Englander-Golden, *J. Chem. Phys.* **43**, 1464 (1965).
23. S. R. Hunter, J. G. Carter, and L. G. Christophorou, *J. Chem. Phys.* **90**, 4879 (1989).
24. R. W. Odom, D. L. Smith, and J. H. Futrell, *J. Phys. B* **8**, 1349 (1975); J. E. Delmore and L. D. Appelhaus, *J. Chem. Phys.* **84**, 6238 (1986).
25. Y. Wang, R. L. Champion, L. D. Doverspike, J. K. Olthoff, and R. J. Van Brunt, *J. Chem. Phys.* **91**, 2254 (1989).
26. A. V. Phelps and R. J. Van Brunt, *J. Appl. Phys.* **64**, 4269 (1988).
27. J. P. Novak and M. F. Fréchet, *J. Appl. Phys.* **55**, 107 (1984).
28. T. Yoshizawa, Y. Sakai, H. Tagashira, and S. Sakamoto, *J. Phys. D* **12**, 1839 (1979).
29. C. Szymkowski and K. Maciag, *Chem. Phys. Lett.* **124**, 463 (1986).
30. M. Zubek, S. Kadifachi, and J. B. Hasted, in *Book of Abstracts of the European Conference on Atomic Physics*, J. Kowalski, G. zu Putlitz, and H. G. Weber, eds., Heidelberg (1981), p. 763.
31. V. F. Sokolov and Y. A. Sokilova, *Sov. Tech. Phys. Lett.* **7**, 268 (1981).
32. O. J. Orient, I. Iger, and S. K. Srivastava, *J. Chem. Phys.* **77**, 3523 (1982).
33. O. J. Orient and S. K. Srivastava, *J. Chem. Phys.* **80**, 140 (1984).
34. L. Vušković and S. Trajmar, *J. Chem. Phys.* **77**, 5436 (1982).
35. L. Sanche and G. J. Schulz, *J. Chem. Phys.* **58**, 79 (1973).
36. L. Andrić, I. M. Čadež, R. I. Hall, and M. Zubek, *J. Phys. B* **16**, 1837 (1983).
37. I. M. Čadež, V. M. Pejčev, and M. V. Kurepa, *J. Phys. D* **16**, 305 (1983).
38. O. J. Orient and S. K. Srivastava, *J. Chem. Phys.* **78**, 2949 (1983).
39. S. M. Spyrou, I. Sauers, and L. G. Christophorou, *J. Chem. Phys.* **84**, 239 (1986).
40. J. Rademacher, L. G. Christophorou, and R. P. Blaunstein, *J. Chem. Soc. Faraday Trans. II*, **71**, 1212 (1975).
41. G. H. Dunn, *Phys. Rev. Lett.* **8**, 62 (1962).
42. T. F. O'Malley and H. S. Taylor, *Phys. Rev.* **176**, 207 (1968).
43. R. J. Van Brunt and L. J. Kieffer, *Phys. Rev. A* **2**, 1899 (1970).
44. J. A. Tossell, *Chem. Phys.* **154**, 211 (1991).
45. A. Benitez, J. H. Moore, and J. A. Tossell, *J. Chem. Phys.* **88**, 6691 (1988).
46. I. Sauers, L. G. Christophorou, and S. M. Spyrou, *Plasma Chem. Plasma Process.*, **13**, 17 (1993).
47. J. S. Wang and J. L. Franklin, *Int. J. Mass. Spectrom. Ion Phys.* **36**, 233 (1980).
48. P. G. Datskos and L. G. Christophorou, *J. Chem. Phys.* **90**, 2626 (1989).
49. P. W. Harland and J. C. J. Thynne, *J. Phys. Chem.* **75**, 3517 (1971).
50. L. M. Babcock and G. E. Streit, *J. Phys. Chem.* **86**, 1240 (1982).
51. T. M. Miller, A. E. S. Miller, and X. Liu, *Abstracts of Contributed Papers, 17th International Conference on the Physics of Electronics and Atomic Collisions*, J. E. McCarthy, W. R. MacGillivray, and M. C. Standage, eds. (1991), p. 260.
52. R. J. Van Brunt, *J. Res. Natl. Bur. Stand.* **90**, 229 (1985); R. J. Van Brunt and M. C. Siddagangappa, *Plasma Chem. Plasma Process.* **8**, 207 (1988).
53. A. Derdouri, J. Casanovas, R. Hergli, R. Grob, and J. Mathieu, *J. Appl. Phys.* **65**, 1852 (1989).
54. I. Sauers, *Plasma Chem. Plasma Process.* **8**, 247 (1988).
55. R. J. Van Brunt and J. T. Herron, *IEEE Trans. Electr. Insul.* **25**, 75 (1990).
56. D. B. Ogle and G. A. Woolsey, *J. Phys. D*, **20**, 453 (1987).
57. C. L. Chen and P. J. Chantry, *J. Chem. Phys.* **71**, 3897 (1979).